

# Cumulative damage for the 28CrMoV5-08 steel under thermomechanical loading

R. El Abdi\* (\*) and H. Samrout#

Laboratoire Génie de Production-Ecole Nationale d'Ingénieurs,  
B. P. 1629. 65016 Tarbes Cedex, FRANCE

## Abstract

*This paper is committed to the study of the damage of the 28CrMoV5-08 steel used in railway brake discs under thermomechanical loading. Isothermal and anisothermal experimental uniaxial cyclical traction/compression tests are given to identify the fatigue damage law and the number of cycles to fracture versus temperature. For a better comprehension of the behavior of this material, metallurgical analyse which were conducted on the samples used in the experimental tests, have indicated the existence of fatigue damage and no microstructural changes.*

## Riassunto

Oggetto del lavoro è la valutazione del danno provocato dal carico termomeccanico all'acciaio 28CrMoV5-08 impiegato per i dischi dei freni ferroviari. Vengono illustrate le prove sperimentali di trazione/compressione cicliche uniassiali isoterme ed anisoterme effettuate allo scopo di individuare la legge del danno dovuto alla fatica, nonché il rapporto tra la temperatura ed il numero di cicli necessari per raggiungere la rottura da fatica. Dai risultati delle analisi metallurgiche eseguite sui campioni utilizzati per le prove sperimentali per meglio comprendere il comportamento di questo acciaio è emersa la presenza di danni da fatica senza alterazioni microstrutturali.

## INTRODUCTION

Structural components working at high temperature under cyclic conditions are the seat of many complex phenomena including thermomechanical as well as metallurgical effects. This is the case of brake discs used in the French T.G.V.s (High Speed Trains) which are subjected simultaneously to mechanical and thermal loadings caused by the pressure of composite material brake pads against the friction surface. At present, the T.G.V.s reach 270 Km/h (168 mph) and are equipped with brake discs of a high resistant steel (28CrMoV5-08). In the future, this speed will surely increase up to 350 Km/h. At this level with the increasing energy dissipated by friction, some problems may appear concerning the capacity of fatigue resistance of such structures. The braking equipment consists of a brake disc and brake pads which function by pressing against the friction area of the disc. The application of the brake pads induce a friction heat flux which is generated into the two components in contact and causes transient thermal gradients.

The high level of transient thermal gradients may induce severe stresses, and local and general plastic strains which cause residual stresses after cooling. Because of the repeated braking, the brake discs suffer damage which causes the apparition of microcracks on the friction area of the disc. Observations made on such brake discs indicated **oligocyclical fatigue damage** (Samrout [1]).

The interaction of physical phenomena is complex; there are thermal exchanges, viscous effects (creep, relaxation, effect of load rate), plastic strain memory effect, thermal expansion, microstructural changes, cyclic softening plus other phenomena such as friction and wear (Nouailhas [2], Kawai [3], Krempf [4]). The aim of our study is to develop an anisothermal fatigue damage model, giving the plastic strain versus the number of cycles to fracture when the temperature varies. The model will be necessary for all extension and/or improvement of the mechanical capacity of brake discs.

(\*) Author to whom correspondence should be addressed

## ON THE EXPERIMENTAL PROCEDURE

The material used in the brake disc is the 28CrMoV5-8 steel. Table I gives the chemical composition of the material. On the basis of experimental results obtained at Ecole des Mines d'Albi Carmaux, cylindrical samples were submitted to uniaxial cyclic loadings (under alternative tension-compression) for a strain ranges  $\Delta\epsilon=1.4\%$  at different temperatures equal to 20°, 200°, 300°, 500° and 600°C with strain speed  $\dot{\epsilon}$  equal to  $10^{-3} \text{ s}^{-1}$ . For each temperature, we had to perform cyclic test run without holding time until rupture.

In opposite to the three-axial loadings which are difficult to control, the uniaxial cyclic loadings are easy to achieve and

to explain. The model deduced from the uniaxial test is sufficient for a good reproduction of the real three dimensional behavior of the material (Ben Cheikh[5])

Fig. 1 gives the stress range ( $\Delta\sigma$ ) versus the cycle number. The decreasing curve shows that the used steel presents a cyclic softening effect (Fig. 1). Table 2 gives different experimental results where  $\Delta\epsilon_{\text{plast.}}$  is the plastic strain range at stabilized cycle. We note a low-cycle fatigue (low number of cycles to failure,  $N_F < 2000$ ) and the number of cycles to fracture  $N_F$  does not vary much until 300°C. It abruptly decreases after this temperature.

**TABLE 1 - Chemical composition of the material**

	Carbon	Chromium	Molybdenum	Vanadium
Composition (%)	0.28	1.25	0.8	$0.2 < x < 0.4$

## PROPOSED ANISOTHERMAL MODEL

In order to make calculations under variable temperature, the Manson-Coffin and Basquin law is choosed (Gilbert [6]):

$$\frac{\Delta\epsilon_{\text{plast.}}}{2} = C(T) * (2N_F)^{B(T)} \quad (1)$$

where  $\Delta\epsilon_{\text{plast.}}$  is the plastic strain range.

Using Table 2, the parameters  $C(T)$  and  $B(T)$  are interpolated by functions of temperature:

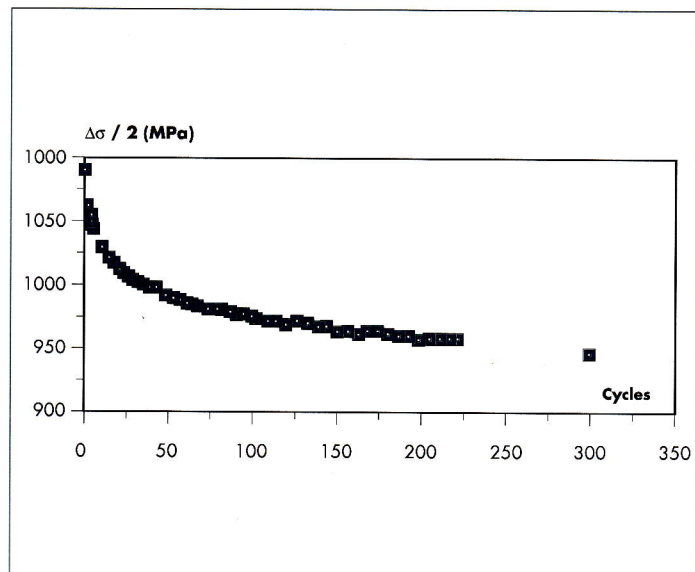


Figure 1: Stress curve for 20°C ( $De = 1.4\%$ )

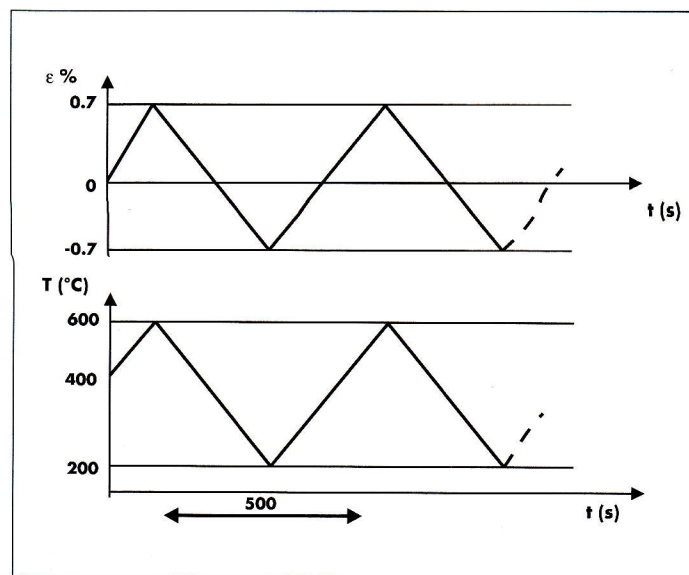


Figure 2: Definition of an in-phase thermomechanical loading

$$C(T) = 284.5 - 3.18 T + 1.29 \cdot 10^{-2} T^2 - 1.33 \cdot 10^{-5} T^3 \quad (2)$$

$$B(T) = -1.046 + 3.72 \cdot 10^{-3} T - 1.51 \cdot 10^{-5} T^2 + 1.51 \cdot 10^{-8} T^3$$

So, we can have the plastic strain variation curve ( $\Delta\epsilon_{\text{plast.}}$ ) versus temperature.

The thermomechanical tests were designed to check the model under cyclical loadings (alternative tension-compression) at variable temperatures ( $200^\circ\text{C} \leq T \leq 600^\circ\text{C}$ ). In the tests both temperature and strain were therefore cyclic. Several types of thermomechanical loadings were used (Samrout [7]). We presented one test as shown in Fig. 2. In Fig. 2, the tempera-



**TABLE 2 - Fatigue results at different temperatures**

Temperature (°C)	E (Young Modulus) GPa	N <sub>F</sub>	$\frac{\Delta\epsilon_{(plast.)}}{2}$ at stabilized cycle
20	186	1497	0,2098%
200	182	1568	0,2099%
300	168	1530	0,21%
500	157	685	0,25%
600	140	488	0,325%

ture is cycled between 200°C and 600°C under conditions of  $\Delta\epsilon = 1.4\%$ . The cyclic thermal loading and applied strain are in-phase.

Fig. 3 gives experimental results (global stress versus global strain) at stabilized cycle. The stabilization of stress occurs rapidly (after approximately 12 cycles). In the vicinity of 200°C, we observed an increasing effect of plasticity due to a temperature delay when decreasing the strain (the experimental temperature is not exactly in-phase with the strain after the first cycle). The number of cycles to fracture is equal to 184. It is less than all the others in the case of isothermal tests (Table 2); the effect of variable temperature considerably reduces the number of the cycles to fracture.

The expression of the strain is the following:

$$\epsilon = \epsilon_e + \epsilon_p \quad (3)$$

where  $\epsilon$  is the total strain,  $\epsilon_e$  is the elastic strain and  $\epsilon_p$  is the viscoplastic strain. The expression of the strain variation is:

$$\Delta\epsilon = \Delta\epsilon_e + \Delta\epsilon_p \quad (4)$$

So, we can write: 
$$\frac{\Delta\epsilon_p}{2} = \frac{\Delta\epsilon}{2} - \frac{\Delta\epsilon_e}{2} \quad (5)$$

In the anisothermal test (fig. 3) the total strain variation  $\Delta\epsilon$  is equal to 1.4%. Elastic strain is deduced from Hooke law:

$$\epsilon_e = \frac{\sigma}{E} \quad (6)$$

where E is the Young modulus (according to the temperature). Fig. 4 gives the comparison between strain deduced from anisothermal test (equ.(4)) and the one deduced from isothermal tests (equ.(1)) when the number of cycles to fracture N<sub>F</sub> is equal to 184. The presented results prove that the proposed anisothermal fatigue damage model is in good agreement with the real behavior of the material used.

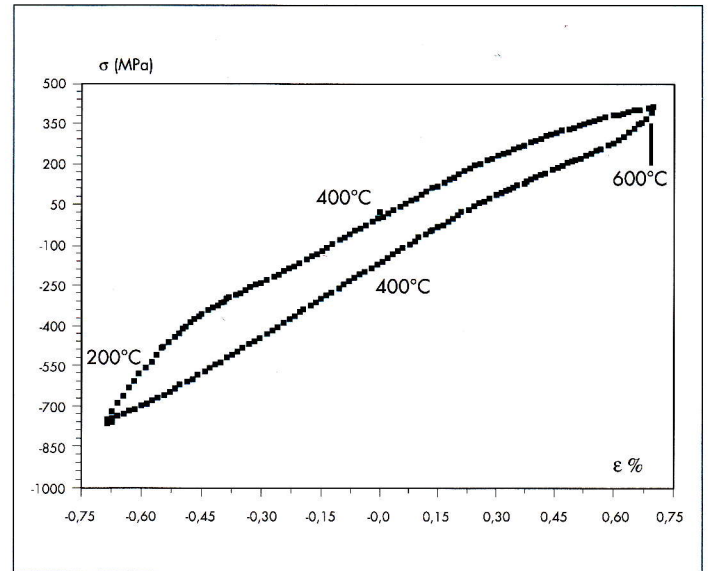


Figure 3: Experimental anisothermal results at stabilized cycle

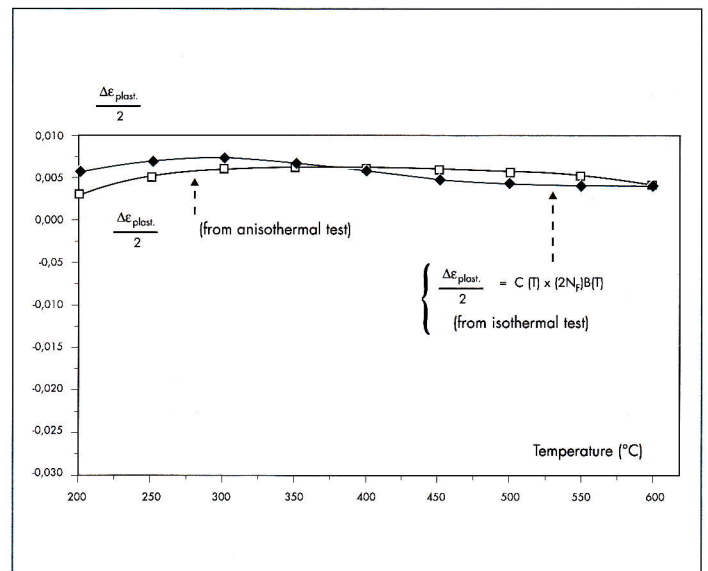


Figure 4: Comparison between the proposed model and the anisothermal results

In Fig. 5, the strain was cycled between -0,4% and 0,4% while the temperature was kept constant at 300°C during a few cycles, then increased to 600°C and decreased back to 300°C. This last test was designed to check the influence of temperature history (Cailletaud[8]) on the behavior of this material by comparing the stress obtained before and after the overheating (or underheating).

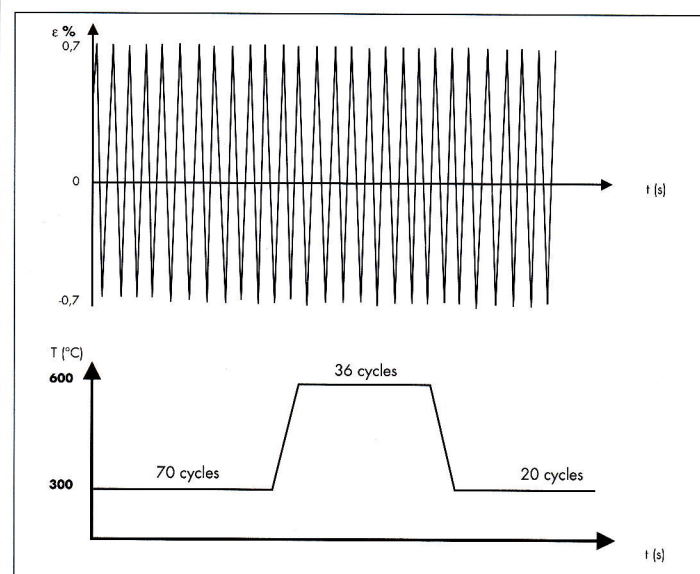


Figure 5: Definition of thermomechanical loading before and after overheating

Fig. 6 gives the stresses versus the cycle number. We observe a minimal difference between the stress obtained at 70th cycle and the stress obtained at 110th cycle. This minimal gap shows that it is not necessary to take the effect of temperature history into account in the proposed model (equ.(1)).

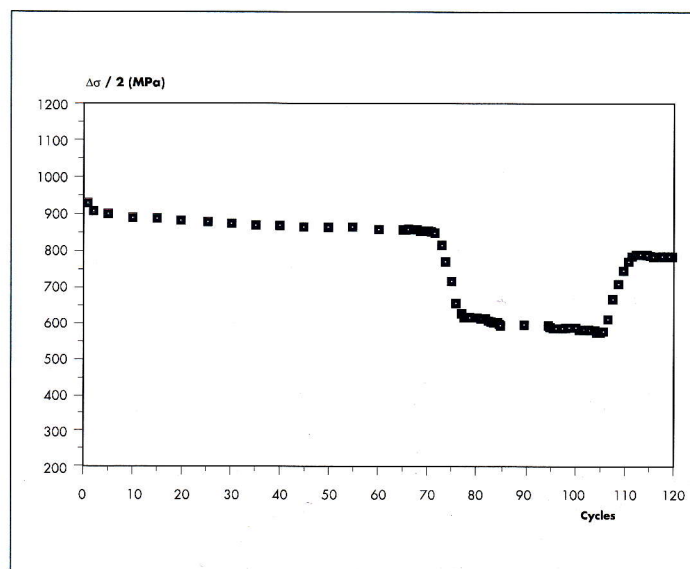


Figure 6: Stress obtained before and after overheating

## METALLURGICAL ANALYSIS

The aim of this paragraph is to perform a complete study of the internal structure of the material (crack propagation modes, the influence of temperature, type of rupture, ...) under isothermal and real conditions of loading. We must therefore perform metallurgical analyse on the specimens extracted from the samples.

The results of the analyse should or should not justify the consideration of some physical phenomena in the model.

### About the hypothesis of microstructural stability

The proposed equation (1) is valid until the steel's tempering point which is 635°C and if there are not metallurgical transformations. Beyond 635°C structural transformations must be included in the model.

The specimens used in the following analysis were extracted from samples which were submitted to isothermal tests.

## Preparation of the specimens

Etching polished metal surfaces with a chemical reagent is a means of differentiating the metal's structural constituents when as is most often the case, they are not readily distinguishable. The usual practice for etching a polished surface is to immerse it in a cold etchant (Nital) for a required period time. The etching is then stopped by washing the specimen with water and drying it rapidly with hot air. This method gives clean metal surfaces which are generally free from all etching debris.

## Analysis under an optical microscope

The object of the micrography is to reveal the internal structure of the alloy, which depends on its crystallography and its constitution. This is why an analysis under a light microscope is necessary for a polished and etched surface.

We have observed inclusions in the material. Their locations are visible in the adjoining Photos where a phenomenon has



turned the surrounding structure black. The microstructure shows no appreciable change at 600°C (see Photos 1 and 2). The observation of the microstructure shows the presence of martensite needles called acicular martensite. Although the martensite needles directions seem to be aleatory, we can

observe a particular orientation inside every initial grain of the austenite (see De Ferri [9]).

All the observations lead to a microstructural stability until 600°C. In fact, we observe the same tempering martensite whatever the temperature or the mechanical loading.

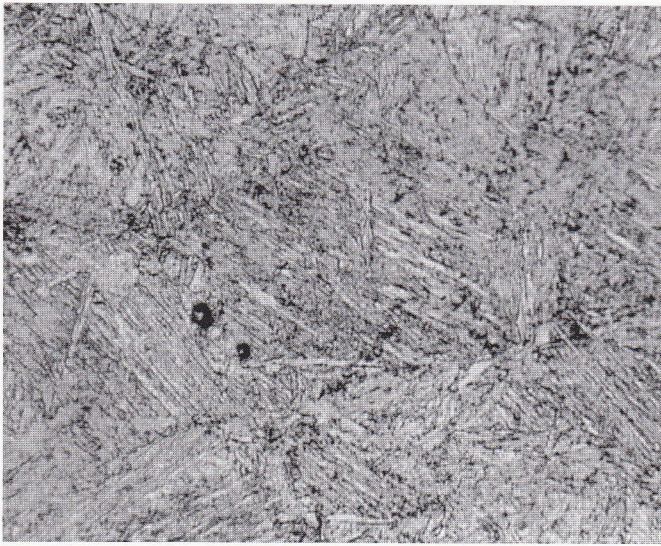


Photo 1: Microstructure after cyclical test at 20°C (X 500)

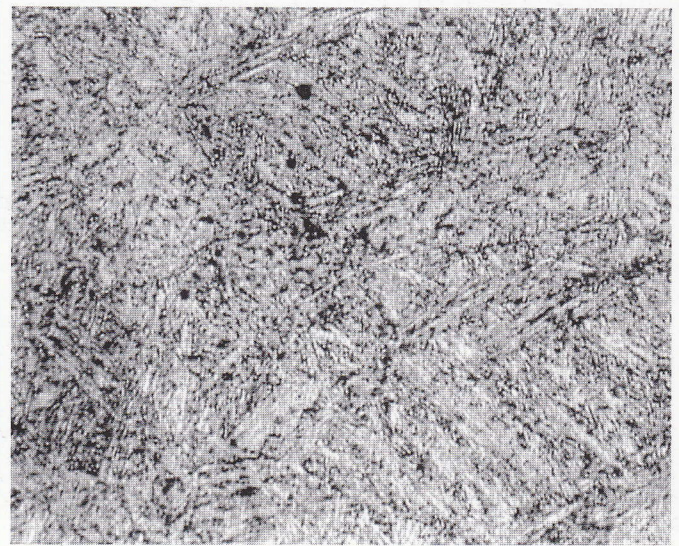


Photo 2: Microstructure after cyclical test at  $\Delta\epsilon = 1.4\%$  at 600°C (X 500)

## STUDY OF RUPTURE FEATURES

### Rupture feature obtained at 600°C

We have analysed the rupture features of all samples. The principal aim of this analysis is to describe the type of damage, the detailed characteristics of the morphology of rupture features and their evolution with temperature.

Photo 3 shows the rupture feature obtained at 600°C for a strain range  $\Delta\epsilon = 1.4\%$ . We observe two different zones; the first zone is in the middle of the feature. It is characteristic of the final rupture of the sample (ductile rupture). All around this zone, we have another smooth zone which characterizes the initiation and propagation of cracks. In this second zone, we observe radial lines which may be due to multiple initiation and propagation of cracks.

This type of feature is similar to a **fatigue rupture** (De Ferri [9]). We have three types of phenomena; the initiation, the slow propagation of cracks and the final rupture. The place of primary initiation of cracks is in the second zone where the width of initiation is major (on the left top and on the right bottom of the feature).

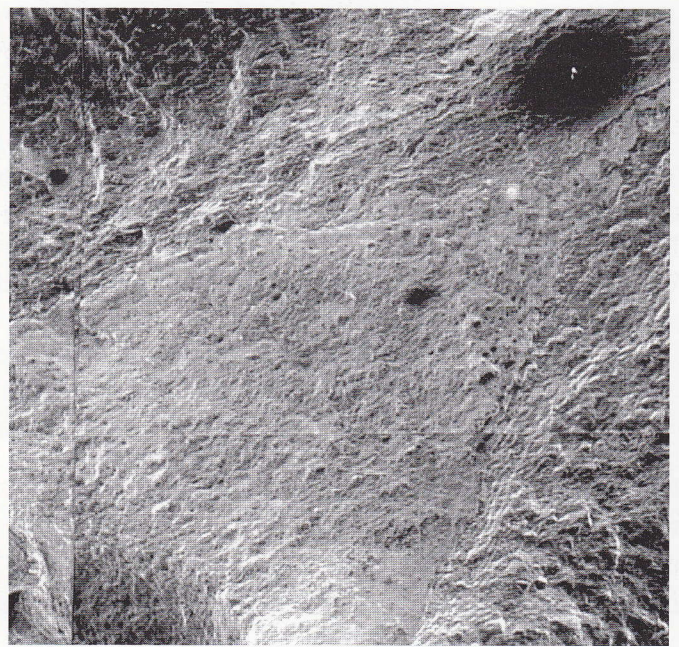


Photo 3: Rupture feature obtained at 600°C (X 15)



## Rupture feature obtained at 200°C

The rupture feature obtained at 200°C (Photo 4) is very different from that obtained at 600°C (Photo 3). The zone of initiation and propagation is difficult to discern around the first zone. We can hardly observe the location of primary initiation of cracks at the left top of the feature.

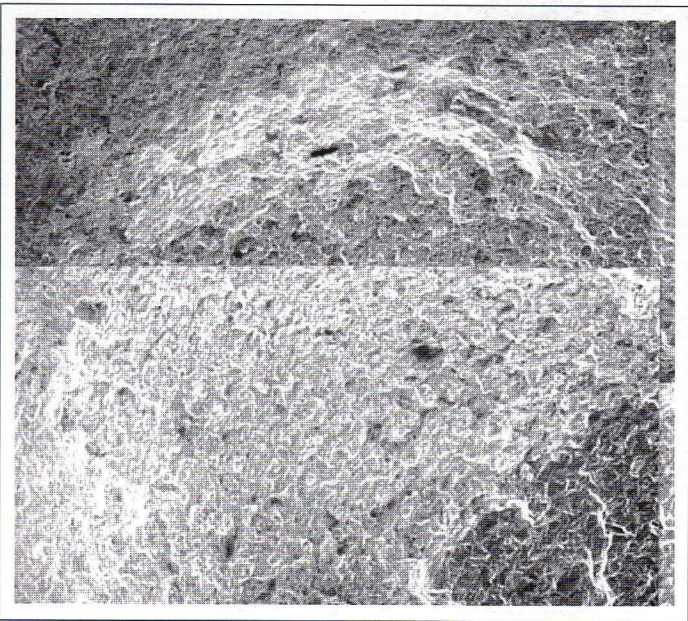


Photo 4: Rupture feature obtained at 200°C (X 15)

## ACKNOWLEDGMENTS

The authors would like to thank the “Ecole des Mines d’Albi Carmaux (France)”, the “Office National d’Etudes et de Recherches Aéropatiales à Châtillon (France)” and the “les Usines Dehousse à Pau (France)” for their cooperation.

## REFERENCES

[1] Samrout, H. Loi de Comportement Elastoviscoplasticité à Température Variable d’un Acier de Disques de Frein pour Matériel Ferroviaire. *Thèse de Doctorat d’Université Bordeaux I*, Décembre 1996.

[2] Nouailhas, D. Unified Modelling of Cyclic Viscoplasticity, Application to Austenitic Stainless Steels. *Int. J. of Plasticity* (1989) Vol. 5, pp. 501-520.

[3] Kawai, M. and Y. Ohashi. Coupled Effect Between Creep and Plasticity of Type 316 Stainless Steel at Elevated Temperature. *2<sup>nd</sup> Int. Conf. on Constitutive Laws for Engineering Materials, Theory and Applications*, Tucson, Arizona, DESAI et al. (eds.), Elsevier 1987.

[4] Krempl, E. and D. Yao. The Viscoplasticity Theory Based on Overstress Applied to Ratchetting and Cyclic Hardening. *2<sup>nd</sup> Int. Conf. on Low-Cycle Fatigue and Elasto-Plastic Behaviour of Materials*. Munich 1984.

## Comparison

The comparison between the feature obtained at 200°C and that obtained at 600°C shows that increasing the temperature encourages the development of the crack propagation zone.

## CONCLUSIONS

This paper presents a anisothermal damage model for the 28CrMov5-08 steel. For a strain range  $\Delta\epsilon=1.4\%$ , isothermal cyclic tests are made for temperatures between 20° and 600°C. Using the parameter values obtained for each temperature, we give an anisothermal fatigue damage model within the temperature range of 20° to 600°C. Experimental tests validate the proposed anisothermal model which is based on the use of the Manson-Coffin model.

Tests using other strain ranges ( $\Delta\epsilon = 1, 1.2, 1.6$  and  $1.8\%$ ) (see Samrout [4]) lead to the same anisothermal damage model.

An anisothermal test where the temperature was kept constant during few cycles while the strain was cycled between  $-0.4\%$  and  $0.4\%$  shows that for the proposed model which is based on the isothermal tests, it is not necessary to take the effect of the temperature history into account.

Metallurgical analyse show no microstructural changes in the material below 600°C. Beyond 635°C which is the steel’s tempering point, structural transformations must be included in the model.

[5] Ben Cheikh, A. Elastoviscoplasticité à température variable. *Thèse de Doctorat, Université de Paris-VI* 1987.

[6] Gilbert, J., M. Lebienvu, G. Pluinage. Fatigue Thermomécanique d’Aciers pour Turbines. *Mémoires et Etudes Scientifiques. Revue de Métallurgie*. Avril 1986 pp. 221-229

[7] Samrout, H., R. El Abdi, C. Levaillant et D. Delagnes. Optimisation des Paramètres de la Loi de Comportement d’un Acier de Disques de Frein Pour Matériel Ferroviaire. *First International Conference on Integrated Design and Manufacturing in Mechanical Engineering*. Nantes, Avril 1996, pp. 937-946.

[8] Cailletaud, G. and J. L. Chaboche. Macroscopic Description of the Microstructural Changes Induced by Varying Temperature : Example of IN100 Cyclic Behavior. *ICM 3*, Cambridge, England, August 1979, Vol. 2, pp. 23-32.

[9] De Ferri. *Metallographia*. Tome II et V. *Presses Académiques Européennes* S. C. 1966, Bruxelles.